

NASA Contractor Report 145357

A SIMULATION MODEL OF THE PLANETARY BOUNDARY LAYER AT KENNEDY SPACE CENTER

AeroChem Research Laboratories, Inc.
Princeton, NJ 08540

B.C. Hwang

**Contract NAS1-14987
March 1978**



National Aeronautics and
Space Administration

Langley Research Center
Hampton, Virginia 23665

1. Report No. NASA Contractor Report 145357		2. Government Accession No.		3. Recipient's Catalog No.	
4. Title and Subtitle A SIMULATION MODEL OF THE PLANETARY BOUNDARY LAYER AT KENNEDY SPACE CENTER				5. Report Date March 1978	
				6. Performing Organization Code	
7. Author(s) BaoChuan Hwang				8. Performing Organization Report No. AeroChem TP-369	
9. Performing Organization Name and Address AeroChem Research Laboratories, Inc. P.O. Box 12 Princeton, NJ 08540				10. Work Unit No.	
				11. Contract or Grant No. NAS1-14987	
12. Sponsoring Agency Name and Address National Aeronautics and Space Administration Washington, DC 20546				13. Type of Report and Period Covered Final - 24: June 1977 to 28 March 1978	
				14. Sponsoring Agency Code	
15. Supplementary Notes					
16. Abstract A simulation model which predicts the behavior of the Atmospheric Boundary Layer has been developed and coded. The model is partially evaluated by comparing it with laboratory measurements and the sounding measurements at Kennedy Space Center. The applicability of such an approach should prove quite widespread.					
17. Key Words (Suggested by Author(s)) Atmospheric Boundary Layer Simulation Second-Order Closure Turbulence				18. Distribution Statement Unclassified - Unlimited	
19. Security Classif. (of this report) Unclassified	20. Security Classif. (of this page) Unclassified	21. No. of Pages 22	22. Price*		

TABLE OF CONTENTS

	<u>Page</u>
SUMMARY.....	1
I. INTRODUCTION.....	2
II. SIMULATED ATMOSPHERIC BOUNDARY LAYER.....	3
A. The Basic Equations.....	3
B. Modeling Assumptions.....	5
C. One-Dimensional Model.....	7
D. The Empirical Constants and Length Scales.....	8
E. Initial and Boundary Conditions.....	9
F. The Grid System and Finite Difference Approximation.....	11
III. MODEL PREDICTIONS.....	15
A. Laboratory Data Comparisons.....	15
B. Sounding Measurement Comparisons.....	15
IV. DISCUSSION AND CONCLUSIONS.....	18
V. REFERENCES.....	20

SUMMARY

A model simulating the atmospheric boundary layer (ABL) at KSC is developed by using a simplified second-order closure scheme. This model predicts the time variations in the ABL of (i) wind velocity and temperature, (ii) inversion layer height, and (iii) turbulent Reynolds stress and temperature flux. Partial verifications of the model were made by comparing it with the wind tunnel measurements conducted by Arya and the regular sounding measurements at KSC on December 10, 1974. Favorable correlations of the temperature profiles can be seen in both comparisons. A disagreement between the predicted wind velocity after 2.5 hours and the actual sounding measurement at that time, in which the eastern component of the wind velocity is stronger than that measured, is caused by using a mandatory stronger stress near the ground as input.

At present, the simulation model ignores (1) the horizontal advection and diffusion, (2) the buoyant force effect of the water within the ABL, and (3) the radiation effects. These neglected dynamic features may be important in some meteorological conditions at KSC. Further investigation on the effects of these dynamic features is needed.

The computer code of this model is stored in the computer facility at NASA/Langley.

I. INTRODUCTION

The objective of this program is to simulate the atmospheric boundary layer (ABL) at Kennedy Space Center using a second-order closure scheme (or mean Reynolds stress scheme). Such simulation will provide the time variations in the ABL of (i) mean physical quantities such as wind velocity and temperature, (ii) inversion layer height, and (iii) mean turbulent Reynolds stress and temperature flux (characteristics of turbulence). These physical/meteorological quantities are required for:

1. Assessing the environmental impact of a rocket launch several hours or even one or two days in advance.
2. Input to diffusion models, e.g., NASA/MDM, for real-time calculations.
3. Calibrating, locating, and orienting measurement instruments for remote sensing/measurements.
4. Studying possible weather modifications due to rocket exhaust.
5. Modeling the atmospheric chemistry in the ABL.
6. Vehicle design and safety analysis.

In addition, this Simulated Atmospheric Boundary Layer (SABL) model can act as a nesting model incorporated in the large-scale forecasting model (e.g., the Limited Area Time Mash Model in the National Weather Service) to forecast local weather.

Progress of this program has been described previously in the first¹ and second² quarterly progress reports. This report presents a summary of this work and discusses additional results obtained in the past two months.

The support from Scott Wagner, Joseph Mathis, and Richard Bendura of NASA/Langley (Environmental Field Measurements Branch; Marine and Applications Technology Division) is gratefully acknowledged.

II. SIMULATED ATMOSPHERIC BOUNDARY LAYER

A. THE BASIC EQUATIONS

The basic equations employed in the simulation model use the following quantities:

virtual temperature

$$\tilde{T}_v = (1 + 0.61 S) \tilde{T}$$

potential temperature

$$\tilde{\theta} = T \left(\frac{\tilde{P}}{\tilde{P}_0} \right)^{0.288}$$

and virtual potential temperature

$$\tilde{\theta}_v = \tilde{\theta} (1 + 0.61 S)$$

where \tilde{T} is the absolute temperature, S the specific humidity, and \tilde{P}_0 the reference pressure (1000 mb). In the above, the tilde refers to instantaneous values, whereas below, the tilde will be removed to indicate mean quantities. Within the ABL, it is adequate to assume that the velocity change, due to variations in the density produced by variations of pressure (but not of temperature), is small. We also assume a constant (both time and spacial independent) \tilde{T}_0 corresponding to $\tilde{\theta}_{0v}$, such that the density of air is described by

$$\tilde{\rho} \cong \tilde{\rho}_0 + \left(\frac{\partial \rho_0}{\partial \tilde{\theta}_v} \right) \tilde{\theta}_{1v} \cong \tilde{\rho}_0 + \beta \tilde{\theta}_{1v}$$

where $\tilde{\theta}_{1v} = \tilde{\theta}_v - \tilde{\theta}_{0v}$ and $\beta = \left(\frac{1}{\tilde{\theta}_v} \right)$ are the coefficients of thermal expansion.

The latter assumption is a strong Boussinesq approximation, permissible for dry air; it is a first-order approximation for including water vapor. Incorporating the above assumptions, the mean equations of motion for the velocity, U , V , and the virtual potential temperature, θ_v , are

$$\frac{\partial U_i}{\partial x_i} = 0 \quad (1)$$

$$\frac{\partial U_i}{\partial t} + \frac{\partial}{\partial x_k} (U_k U_i + \overline{u_k u_i}) + \epsilon_{jkl} f_k U_l = - \frac{\partial P}{\partial x_j} - g_j \beta \theta_v + \nu \nabla^2 U_j \quad (2)$$

$$\frac{\partial \theta_v}{\partial t} + \frac{\partial}{\partial x_k} (U_k \theta_v + \overline{u_k \theta}) = \alpha \nabla^2 \theta_v \quad (3)$$

where P is the mean kinematic pressure, $g_j = (0, 0, -g)$ the gravitation vector, $f_j = (0, 0, f)$ the Coriolis parameter, ν the kinematic viscosity, and α the thermal diffusivity. The overbars represent ensemble averages; the lower case terms are the fluctuation components and are governed by (subtracting the equation of motion from the mean Eqs. (1) to (3))

$$\frac{\partial u_i}{\partial x_i} = 0 \quad (4)$$

$$\frac{\partial u_j}{\partial t} + \frac{\partial}{\partial x_k} (u_k u_j + u_j u_k + \overline{u_k u_j}) + \epsilon_{jkl} f_k u_l = -\frac{\partial p}{\partial x_j} - g_j \theta + \nu \nabla^2 u_j \quad (5)$$

$$\frac{\partial \theta}{\partial t} + \frac{\partial}{\partial x_k} (\theta u_k + u_k \theta + \overline{u_k \theta}) = \alpha \nabla^2 \theta \quad (6)$$

Since the mean Eqs. (1) to (3) involve the Reynolds stress $\overline{u_i u_j}$ and the heat flux term $\overline{u_i \theta}$, the mean equations are closed by introducing the equations for the Reynolds stress and heat flux from Eqs. (5) and (6),

$$\begin{aligned} \frac{\partial \overline{u_i u_j}}{\partial t} + \left[\frac{\partial}{\partial x_k} \overline{u_k u_i u_j} + \overline{u_k u_i u_j} - \nu \frac{\partial}{\partial x_k} \overline{u_i u_j} \right] + \frac{\partial}{\partial x_j} \overline{p u_i} \\ + \frac{\partial}{\partial x_i} \overline{p u_j} + f_k (\epsilon_{jkl} \overline{u_l u_i} + \epsilon_{ikl} \overline{u_l u_j}) \\ = -\overline{u_k u_i} \frac{\partial u_j}{\partial x_k} - \overline{u_k u_j} \frac{\partial u_i}{\partial x_k} - \beta (g_j \overline{u_i \theta} + g_i \overline{u_j \theta}) \\ + \overline{p \left(\frac{\partial u_i}{\partial x_j} + \frac{\partial u_j}{\partial x_i} \right)} - 2\nu \overline{\frac{\partial u_i}{\partial x_k} \frac{\partial u_j}{\partial x_k}} \end{aligned} \quad (7)$$

$$\begin{aligned} \frac{\partial \overline{u_j \theta}}{\partial t} + \frac{\partial}{\partial x_k} \left(\overline{u_k \theta u_j} + \overline{u_k u_j \theta} \right) - \alpha \overline{u_j} \frac{\partial \theta}{\partial x_k} - \nu \overline{\theta} \frac{\partial u_j}{\partial x_k} + \frac{\partial}{\partial x_j} \overline{p \theta} + \epsilon_{jkl} f_k \overline{u_l \theta} \\ = -\overline{u_j u_k} \frac{\partial \theta}{\partial x_k} - \overline{\theta u_k} \frac{\partial u_j}{\partial x_k} - \beta g_j \overline{\theta^2} + \overline{p} \frac{\partial \theta}{\partial x_j} - (\alpha + \nu) \overline{\frac{\partial u_j}{\partial x_k} \frac{\partial \theta}{\partial x_k}} \end{aligned} \quad (8)$$

$$\overline{\frac{\partial \theta^2}{\partial \tau}} + \frac{\partial}{\partial x_k} \overline{u_k \theta^2} + \overline{u_k \theta^2} - \alpha \overline{\frac{\partial \theta^2}{\partial x_k}} = -2 \overline{u_k \theta} \frac{\partial \theta}{\partial x_k} - 2\alpha \overline{\frac{\partial \theta}{\partial x_k} \frac{\partial \theta}{\partial x_k}} \quad (9)$$

B. MODELING ASSUMPTIONS

Since the higher order terms, the diffusion terms $\overline{u_i u_j u_k}$ and $\overline{u_i u_j \theta}$ and the terms including the fluctuation of pressure, e.g.,

$\overline{p \left(\frac{\partial u_i}{\partial x_j} + \frac{\partial u_j}{\partial x_i} \right)}$ (usually called the energy redistribution terms), are involved

in Eqs. (7) to (9), these unknowns must be modeled if one does not intend to invoke a higher order closure scheme. The models adopted for these terms are based on the works of Rotta,³ Kolmogoroff,⁴ and Mellor and Herring.⁵ They are

$$\overline{p \left(\frac{\partial u_i}{\partial x_j} + \frac{\partial u_j}{\partial x_i} \right)} = -\frac{q}{3\ell_1} \left(\overline{u_i u_j} - \frac{\delta_{ij}}{3} q^2 \right) + Cq^2 \left(\frac{\partial u_i}{\partial x_j} + \frac{\partial u_j}{\partial x_i} \right) \quad (10)$$

$$\overline{p \frac{\partial \theta}{\partial x_j}} = \frac{q}{3\ell_2} \overline{u_j \theta} \quad (11)$$

$$2\nu \overline{\frac{\partial u_k}{\partial x_k} \frac{\partial u_j}{\partial x_k}} = \frac{2}{3} \frac{q^3}{\Lambda_1} \delta_{ij} \quad (12)$$

$$(\alpha + \nu) \overline{\frac{\partial u_j}{\partial x_k} \frac{\partial \theta}{\partial x_k}} = 0 \quad (13)$$

$$2\alpha \overline{\frac{\partial \theta}{\partial x_k} \frac{\partial \theta}{\partial x_k}} = 2 \frac{q}{\Lambda_2} \overline{\theta^2} \quad (14)$$

$$\overline{u_k u_i u_j} = -q\lambda_1 \left(\overline{\frac{\partial u_i u_j}{\partial x_k}} + \overline{\frac{\partial u_i u_k}{\partial x_j}} + \overline{\frac{\partial u_j u_k}{\partial x_i}} \right) \quad (15)$$

$$\overline{u_k u_j \theta} = -q\lambda_2 \left(\overline{\frac{\partial u_k \theta}{\partial x_j}} + \overline{\frac{\partial u_j \theta}{\partial x_k}} \right) \quad (16)$$

$$\overline{u_k \theta^2} = -q\lambda_3 \frac{\partial \theta^2}{\partial x_k} \quad (17)$$

$$\overline{pu_1} = \overline{p\theta} = 0 \quad (18)$$

where q^2 is twice the turbulent kinetic energy, $\overline{u^2} + \overline{v^2} + \overline{w^2}$. Substituting Eqs. (10) to (18) into Eqs. (7) to (9) gives

$$\begin{aligned} \frac{D\overline{u_1 u_j}}{Dt} + f_k (\epsilon_{jkl} \overline{u_l u_1} + \epsilon_{ikl} \overline{u_l u_j}) &= \frac{\partial}{\partial x_k} \left[q\lambda_1 \left(\frac{\partial \overline{u_1 u_j}}{\partial x_k} + \frac{\partial \overline{u_1 u_k}}{\partial x_j} + \frac{\partial \overline{u_j u_k}}{\partial x_1} \right) \right. \\ &\quad \left. + v \frac{\partial \overline{u_1 u_j}}{\partial x_k} \right] - \overline{u_k u_j} \frac{\partial u_1}{\partial x_k} - \overline{u_k u_1} \frac{\partial u_j}{\partial x_k} - \beta (g_j \overline{u_1 \theta} + g_1 \overline{u_j \theta}) \\ &\quad - \frac{q}{3\lambda_1} \left(\overline{u_1 u_j} - \frac{\delta_{1j}}{3} q^2 \right) + Cq^2 \left(\frac{\partial u_1}{\partial x_j} + \frac{\partial u_j}{\partial x_1} \right) - \frac{2}{3} \frac{q^3}{\Lambda_1} \delta_{1j} \end{aligned} \quad (19)$$

$$\begin{aligned} \frac{D\overline{u_j \theta}}{Dt} + f_k \epsilon_{jkl} \overline{u_l \theta} &= \frac{\partial}{\partial x_k} \left[q\lambda_2 \left(\frac{\partial \overline{u_j \theta}}{\partial x_k} + \frac{\partial \overline{u_k \theta}}{\partial x_j} \right) + \overline{u_j} \frac{\partial \theta}{\partial x_k} + v\theta \frac{\partial u_j}{\partial x_k} \right] \\ &\quad - \overline{u_j u_k} \frac{\partial \theta}{\partial x_k} - \overline{\theta u_k} \frac{\partial u_j}{\partial x_k} - \beta g_j \overline{\theta^2} - \frac{q}{3\lambda_2} \overline{u_j \theta} \end{aligned} \quad (20)$$

$$\frac{D\overline{\theta^2}}{Dt} = \frac{\partial}{\partial x_k} \left[q\lambda_3 \frac{\partial \overline{\theta^2}}{\partial x_k} + \alpha \frac{\partial \overline{\theta^2}}{\partial x_k} \right] - 2\overline{u_k \theta} \frac{\partial \theta}{\partial x_k} - 2 \frac{q}{\Lambda_2} \overline{\theta^2} \quad (21)$$

Although Eqs. (1) to (3) and (19) to (21) represent a closed second-order system, they are still too complicated to solve. The present program adopts a simplified model based on the so-called "level 3 model" by Mellor and Yamada,⁶ in which the off-diagonal turbulent diffusion and advection of Reynolds stress and flux terms were ignored using the order of magnitude argument. Such a simplified model has been shown to give a favorable comparison with the Wangara experimental results.⁷

C. ONE-DIMENSIONAL MODEL

The one-dimensional simplified second-order closure system we plan to solve is

$$\frac{\partial U}{\partial t} = fV - fV_g + \frac{\partial}{\partial z} (-\overline{uv}) \quad (22)$$

$$\frac{\partial V}{\partial t} = -fU + fU_g + \frac{\partial}{\partial z} (-\overline{vw}) \quad (23)$$

$$\frac{\partial \theta_v}{\partial t} = \frac{\partial}{\partial z} (-\overline{w\theta}) + \frac{fT_v}{g} \left(v \frac{\partial U_g}{\partial z} - u \frac{\partial V_g}{\partial z} \right) - w \frac{\partial \theta_v}{\partial z} + \sigma_r \quad (24)$$

$$\frac{\partial}{\partial t} \left(\frac{q^2}{2} \right) - \frac{\partial}{\partial z} \left[\frac{5}{3} \lambda_1 q \frac{\partial}{\partial z} \left(\frac{q^2}{2} \right) \right] = -\overline{uw} \frac{\partial U}{\partial z} - \overline{vw} \frac{\partial V}{\partial z} + \beta g w \overline{\theta} \frac{q^3}{\Lambda_1} \quad (25)$$

$$\frac{\partial}{\partial t} \left(\frac{\overline{\theta^2}}{2} \right) - \frac{\partial}{\partial z} \left[\lambda_3 q \frac{\partial}{\partial z} \left(\frac{\overline{\theta^2}}{2} \right) \right] = -\overline{w\theta} \frac{\partial \theta_v}{\partial z} - q \frac{\overline{\theta^2}}{\Lambda_2} \quad (26)$$

$$\begin{bmatrix} \overline{u^2} \\ \overline{v^2} \\ \overline{w^2} \end{bmatrix} = \frac{q^2}{3} \begin{bmatrix} 1 \\ 1 \\ 1 \end{bmatrix} + \frac{\ell_1}{q} \begin{bmatrix} 4P_{xx} - 2P_{yy} - 2\beta g w \overline{\theta} \\ -2P_{xx} + 4P_{yy} - 2\beta g w \overline{\theta} \\ -2P_{xx} - 2P_{yy} + 4\beta g w \overline{\theta} \end{bmatrix} \quad (27)$$

$$- \begin{bmatrix} \overline{uv} \\ \overline{uw} \\ \overline{vw} \end{bmatrix} = 3 \frac{\ell_1}{q} \begin{bmatrix} P_{yx} + P_{xy} \\ (\overline{w^2} - cq^2) \frac{\partial U}{\partial z} - \beta g u \overline{\theta} \\ (\overline{w^2} - cq^2) \frac{\partial V}{\partial z} - \beta g v \overline{\theta} \end{bmatrix} \quad (28)$$

$$- \begin{bmatrix} \overline{u\theta} \\ \overline{v\theta} \\ \overline{w\theta} \end{bmatrix} = 3 \frac{\ell_2}{q} \begin{bmatrix} \overline{uw} \frac{\partial \theta_v}{\partial z} + \overline{w\theta} \frac{\partial U}{\partial z} \\ \overline{vw} \frac{\partial \theta_v}{\partial z} + \overline{w\theta} \frac{\partial V}{\partial z} \\ \overline{w^2} - \frac{\partial \theta_v}{\partial z} - \beta g \overline{\theta^2} \end{bmatrix} \quad (29)$$

In the above expressions, $P_{xx} = - \overline{uw} \frac{\partial U}{\partial z}$, $P_{yy} = - \overline{vw} \frac{\partial V}{\partial z}$, and $P_{xy} = - \overline{uw} \frac{\partial V}{\partial z}$. The Coriolis terms have been excluded in the turbulence equations; they may be shown to be small in the ABL.

In practical geophysical fluid dynamics problems, the eddy viscosity K_M and eddy conductivity K_H are often used and are defined as

$$(-\overline{uw}, -\overline{vw}) = K_M \left(\frac{\partial U}{\partial z}, \frac{\partial V}{\partial z} \right) \quad (30)$$

$$-\overline{w\theta} = K_H \frac{\partial \theta_v}{\partial z} \quad (31)$$

Using Eqs. (27) to (29), K_M and K_H can be expressed as

$$K_M = q \ell S_M$$

$$K_H = q \ell S_H$$

where

$$S_M = \frac{3A_1(\overline{w^2} - C_1 q^2)/q^2 + 9A_1 A_2 \ell \beta g \overline{w\theta}/q^3}{1 + 9A_1 A_2 \ell^2 \beta g (\partial \theta_v / \partial z)/q^2}$$

$$S_H = \frac{2A_2 \overline{w^2}/q^2}{1 + 3A_2 B_2 \ell^2 \beta g (\partial \theta_v / \partial z) q^2}$$

and $\overline{w^2}$ is given by Eq. (27).

D. THE EMPIRICAL CONSTANTS AND LENGTH SCALES

The length scales (ℓ_1 , Λ_1 , ℓ_2 , Λ_2) incorporated in the model are assumed to be proportional to a master length scale ℓ , i.e.,

$$(\ell_1, \Lambda_1, \ell_2, \Lambda_2) = (A_1, B_1, A_2, B_2)\ell$$

Although this assumption has not yet been verified, several studies by Mellor and Yamada⁸ indicate that it may be viable. The constants A_1 , B_1 , A_2 , B_2 , and C should be determined from data. The present program, employing the values given by Mellor and Yamada,⁸ gives

$$(A_1, B_1, A_2, B_2, C) = (0.74, 16.6, 0.92, 10.1, 0.08)$$

These values were determined⁸ by matching the turbulent characteristics of the measured neutral stratified wall data to the corresponding values in the model. Local equilibrium was assumed in interpreting the values obtained.

The master scale, ℓ , is determined by solving the equation

$$\begin{aligned} \frac{D}{Dt} (q^2 \ell) - \frac{\partial}{\partial z} \left[\frac{1}{5} q \ell \frac{\partial}{\partial z} (q^2 \ell) \right] &= \ell (1.8) \left[P_{xx} + P_{yy} + \beta g \overline{w\theta} \right] \\ &- \frac{q^3}{B_1} \left\{ 1 + 1.33 \left(\frac{\ell}{kz} \right)^2 \right\} \end{aligned} \quad (32)$$

While one cannot place great confidence in Eq. (32), an alternative for determining ℓ can be used,⁹

$$\begin{aligned} \ell &= \frac{kz}{1 + \frac{kz}{\lambda}} \\ \lambda &= \frac{2.7 \times 10^{-4} V_g}{f} \end{aligned}$$

where V_g is the geostrophic wind speed and k is the Von Karman constant.

E. INITIAL AND BOUNDARY CONDITIONS

The initial value for the mean quantities U , V , and Θ_v for the one-dimensional model can be taken from direct rawinsonde data. Initial values for the turbulence moments q^2 and $\overline{\theta^2}$ are given by invoking local equilibrium, i.e., that the total production balances the dissipation. Therefore we have, from Eq. (25),

$$\frac{q^3}{\Lambda_1} = -\overline{uw} \frac{\partial U}{\partial z} - \overline{vw} \frac{\partial V}{\partial z} + \beta g \overline{w\theta} \quad (33)$$

and

$$\frac{q \overline{\theta^2}}{\Lambda_2} = -\overline{w\theta} \frac{\partial \Theta_v}{\partial z} \quad (34)$$

Solving the algebraic Eqs. (33), (34), (27), (28), (29) and again employing expressions (31) and (32) we obtain

$$- (\overline{uw}, \overline{vw}) = \ell_q S_M \left(\frac{\partial U}{\partial z}, \frac{\partial V}{\partial z} \right) \quad (35)$$

$$- \overline{w\theta} = \ell_q S_H \frac{\partial \theta}{\partial z} \quad (36)$$

$$S_M = 3A_1 \frac{\gamma_1 - C - (6A_1 + 3A_2)\Gamma/B_1}{\gamma_1 - \gamma_2\Gamma + 3A_1\Gamma/B_1} (\gamma_1 - \gamma_2\Gamma)$$

$$S_H = 3A_2 (\gamma_1 - \gamma_2\Gamma)$$

where

$$\gamma_1 = \frac{1}{3} - (2A_1/B_1)$$

$$\gamma_2 = (B_2/B_1) + (6A_1/B_1)$$

$$\Gamma \equiv R_f / (1 - R_f)$$

In these expressions, R_f is the flux Richardson number, i.e.,

$$R_f \equiv - \beta g \overline{w\theta} / (P_{xx} + P_{yy})$$

The flux Richardson number can be related to gradient Richardson, $R_1 =$

$$\beta g \left(\frac{\partial \theta}{\partial z} \right) / \left[\left(\frac{\partial V}{\partial z} \right)^2 + \left(\frac{\partial U}{\partial z} \right)^2 \right] \text{ as}$$

$$R_f = \frac{S_H}{S_M} R_1 = P_{rt}^{-1} R_1$$

where $P_{rt} = \frac{S_M}{S_H}$ is the turbulent Prandtl number.

The surface boundary conditions for U and V satisfy the neutral flow relations

$$(U, V) = (\cos \xi, \sin \xi) \frac{u_*}{k} \ln z/z_0 \quad (37)$$

where $u_* = [(-\overline{uw})^2 + (-\overline{vw})^2]_{z=0}^{1/4}$ is the surface friction velocity and ξ is the angle of the surface friction velocity.

Based on Eq. (37) the following relation is used in the program for the surface condition of U and V

$$(U_1, V_1) = (U_2, V_2) \frac{\ln(z_1/z_0)}{\ln(z_2/z_0)}$$

The surface boundary conditions for the Θ_v are set to be either

$$\Theta_v = \Theta_v(z = 0)$$

or

$$K_H \left(\frac{\partial \Theta_v}{\partial z} \right)_{z=0} = (\overline{w\theta})_{z=0}$$

The surface boundary conditions for q^2 and $\overline{\theta^2}$ determined from Ref. 8 are employed, i.e.,

$$q^2(0) = B_1^{2/3} u_*^2$$

$$\overline{\theta^2}(0) = \frac{(\overline{w\theta})^2}{u_*^2} \frac{B_2}{B_1^{1/3}} P_{rt}$$

The upper boundary conditions for U , V , Θ_v , q , and $\overline{\theta^2}$ are

$$\frac{\partial}{\partial z}(U, V) = 0$$

$$\frac{\partial \Theta_v}{\partial z} = F$$

and

$$q^2(h) = \overline{\theta^2}(h) = 0$$

where F ($K^\circ m^{-1}$) is the observation value of the virtual potential temperature gradient.

F. THE GRID SYSTEM AND FINITE DIFFERENCE APPROXIMATION

Since (1) the master length scale ℓ is proportional to z near the surface but tends toward a constant away from the surface and (2) an accurate computation requires a coordinate system such that $\frac{\Delta z}{\ell} = \text{const.}$, we choose a grid system $\{z_n\}$ so that

$$\Delta z = \Delta \ln z_n \quad \text{for lower portion of the ABL}$$

$$\Delta z = \Delta z_n \quad \text{for upper portion of the ABL}$$

Table I shows the 40 point distribution as an example of the chosen grid system.

TABLE I
THE SELECTED FORTY POINT GRID SYSTEM
Boundary Layer Height Assumed = 2500 m

<u>Grid Index</u> <u>n</u>	<u>Height</u> <u>Z (m)</u>	<u>Grid Index</u> <u>n</u>	<u>Height</u> <u>Z (m)</u>
1	0.0	21	1015.6
2	0.6	22	1093.8
3	1.2	23	1171.9
4	2.4	24	1250.0
5	4.9	25	1328.1
6	9.8	26	1406.3
7	19.5	27	1484.4
8	39.0	28	1562.5
9	78.1	29	1640.6
10	156.3	30	1718.8
11	234.4	31	1796.9
12	312.5	32	1875.0
13	390.6	33	1953.1
14	468.8	34	2031.3
15	546.9	35	2109.4
16	625.0	36	2187.5
17	703.1	37	2265.6
18	781.3	38	2343.8
19	859.4	39	2421.9
20	937.5	40	2500.0

The differential equations we plan to solve are (22) to (26) and (32). They can be reduced to a general expression given by

$$\frac{\partial \phi}{\partial t} = \frac{\partial}{\partial z} \left(P_1 \frac{\partial \phi}{\partial z} \right) - P_2 \frac{\partial \phi}{\partial z} - P_3 \phi + P_4 \quad (38)$$

Table II indicates ϕ , P_1 , P_2 , P_3 , P_4 for Eqs. (22) to (26) and (32).

TABLE II
IDENTIFICATION OF THE VARIABLE ϕ
AND THE PARAMETERS P_1 - P_4 IN EQ. (38)

Eq.	ϕ	P_1	P_2	P_3	P_4
(22, 23)	\hat{V}	K_M	0	if	if \hat{V}_g
(24)	θ_v	K_H	W	0	$\frac{fT_v}{g} \left(v \frac{\partial U_g}{\partial z} - U \frac{\partial v_g}{\partial z} \right) + \sigma_r$
(25)	$\frac{q^2}{2}$	$\frac{5}{3} q \lambda_1$	0	$2 \frac{q}{\Lambda_1}$	$- \overline{uw} \frac{\partial U}{\partial z} - \overline{vw} \frac{\partial V}{\partial z} + \beta g \overline{w\theta}$
(26)	$\frac{\overline{\theta^2}}{2}$	$q \lambda_3$	0	$2 \frac{q}{\Lambda_1}$	$- \overline{w\theta} \frac{\partial \theta_v}{\partial z}$
(32)	$q^2 \ell$	$\frac{1}{5} q \ell$	0	0	$1.8 \ell \left[P_{xx} + P_{yy} + \rho g \overline{w\theta} \right]$ $- \frac{q^3}{B_1} \left\{ 1 + 1.33 \left(\frac{\ell}{kz} \right)^2 \right\}$

The leapfrog finite difference expression for Eq. (38) is

$$\begin{aligned} \frac{\phi_j^{k+1} - \phi_j^{k-1}}{2\Delta t} = & \frac{1}{2(\Delta z)^2} \left\{ \phi_{j+1}^{k+1} \left[(P_1)_j^k + (P_1)_{j+1}^k \right] - \phi_j^{k+1} \left[(P_1)_{j+1}^k \right. \right. \\ & \left. \left. + 2(P_1)_j^k + (P_1)_{j-1}^k \right] + \phi_{j-1}^{k+1} \left[(P_1)_j^k + (P_1)_{j-1}^k \right] \right\} \\ & - \frac{1}{2\Delta z} (P_2)_j^k \left[\phi_{j+1}^{k+1} - \phi_{j-1}^{k+1} \right] - (P_3)_j^k \phi_j^{k+1} + (P_4)_j^k \end{aligned} \quad (39)$$

The finite difference expression (39) can be rewritten as

$$\begin{bmatrix} B_1, A_1, 0, \dots, 0 \\ C_2, B_2, A_2, 0, \dots, 0 \\ \cdot & \cdot & & & \\ \cdot & & \cdot & & \\ \cdot & & & \cdot & \\ \cdot & & & & C_N, B_N \end{bmatrix} \begin{bmatrix} \phi_1^{k+1} \\ \cdot \\ \cdot \\ \cdot \\ \phi_N^{k+1} \end{bmatrix} = \begin{bmatrix} \phi_1^{k-1} + 2\Delta t (P_4)_1^k \\ \cdot & \cdot \\ \cdot & \cdot \\ \cdot & \cdot \\ \phi_N^{k-1} + 2\Delta t (P_4)_N^k \end{bmatrix} \quad (40)$$

The matrix form (40) can easily be solved by using the Thomas algorithm to give

$$\phi_N^{k+1} = V_N$$

and

$$\phi_j^{k+1} = V_j + S_j \phi_{j+1}^{k+1} \quad \text{for } j < N$$

where

$$V_1 = \frac{-\frac{\phi_1^{k-1}}{2\Delta t} + (P_4)_1^k}{B_1}$$

and

$$V_j = \frac{-\frac{\phi_j^{k-1}}{2\Delta t} - (P_4)_j^k + C_j V_{j-1}}{-(B_j + C_j S_{j-1})} \quad \text{for } 1 < j \leq N$$

also

$$S_1 = \frac{-A_1}{B_1}$$

and

$$S_j = \frac{A_j}{-(B_j + C_j S_{j-1})} \quad 1 < j \leq N$$

III. MODEL PREDICTIONS

The model has been partially evaluated by comparing it with two sets of data, the laboratory measurements carried out by Arya¹⁰ and the regular sounding measurements at KSC on December 10, 1974. They are discussed individually below.

A. LABORATORY DATA COMPARISONS

A wind tunnel simulation of a stably stratified surface layer¹⁰ was used for comparison because (1) it provides a complete data set including turbulence information and (2) the turbulence behavior of a laboratory simulated surface layer is less complex than that of an atmospheric boundary layer in nature. The temperature profile calculated using the model will be compared with the measured profile. Based on Eqs. (35) and (36), the temperature profile is related to the velocity profile by

$$\frac{\partial \theta}{\partial z} = \frac{\overline{w\theta}}{\overline{uw}} \text{Pr}_t \frac{\partial U}{\partial z} \quad (41)$$

Since the heat flux and the shear stress are approximately constant in the surface layer, the temperature profile can be easily obtained by integrating Eq. (41) with the given velocity profile and the turbulent Prandtl number. The turbulent Prandtl number in Eq. (41) is dependent upon the gradient Richardson number as deduced from the model described in Section II.E. Using the turbulent Prandtl number from the model and the measured values for the velocity profile, heat flux, and shear stress, a comparison was made of the calculated and measured temperature profiles as shown in Fig. 1. The correlation appears very good. The comparison is restricted to between $0.2 Z_i$ and $0.8 Z_i$, where Z_i is the surface layer height, because the laboratory data show approximately constant flux and constant stress in this range only.

B. SOUNDING MEASUREMENT COMPARISONS

Since the stationary state, the equilibrium state, the constant stress, and the constant flux in the laboratory-simulated surface layer rarely exist in the natural ABL, the model is used to make a calculation and to compare it with the existing measured data in an ABL. Such comparisons will also guide further refinements of the model. A theoretical calculation using the model for the physical quantities in the ABL of KSC over a three hour period during the night of December 10, 1974 was made. The resultant wind velocities and temperatures are compared with the available sounding data in Fig. 2.

A satisfactory agreement for the temperature and the southern component of the wind velocity, V , can be seen in the figure. On the other hand, the predicted value of the eastern component of the velocity, U , exceeds the measured value. This causes an error of about 20° in the predicted wind direction toward the east and a factor of 2 greater predicted than measured wind speed. Further discussion of this disagreement is given in the following section.

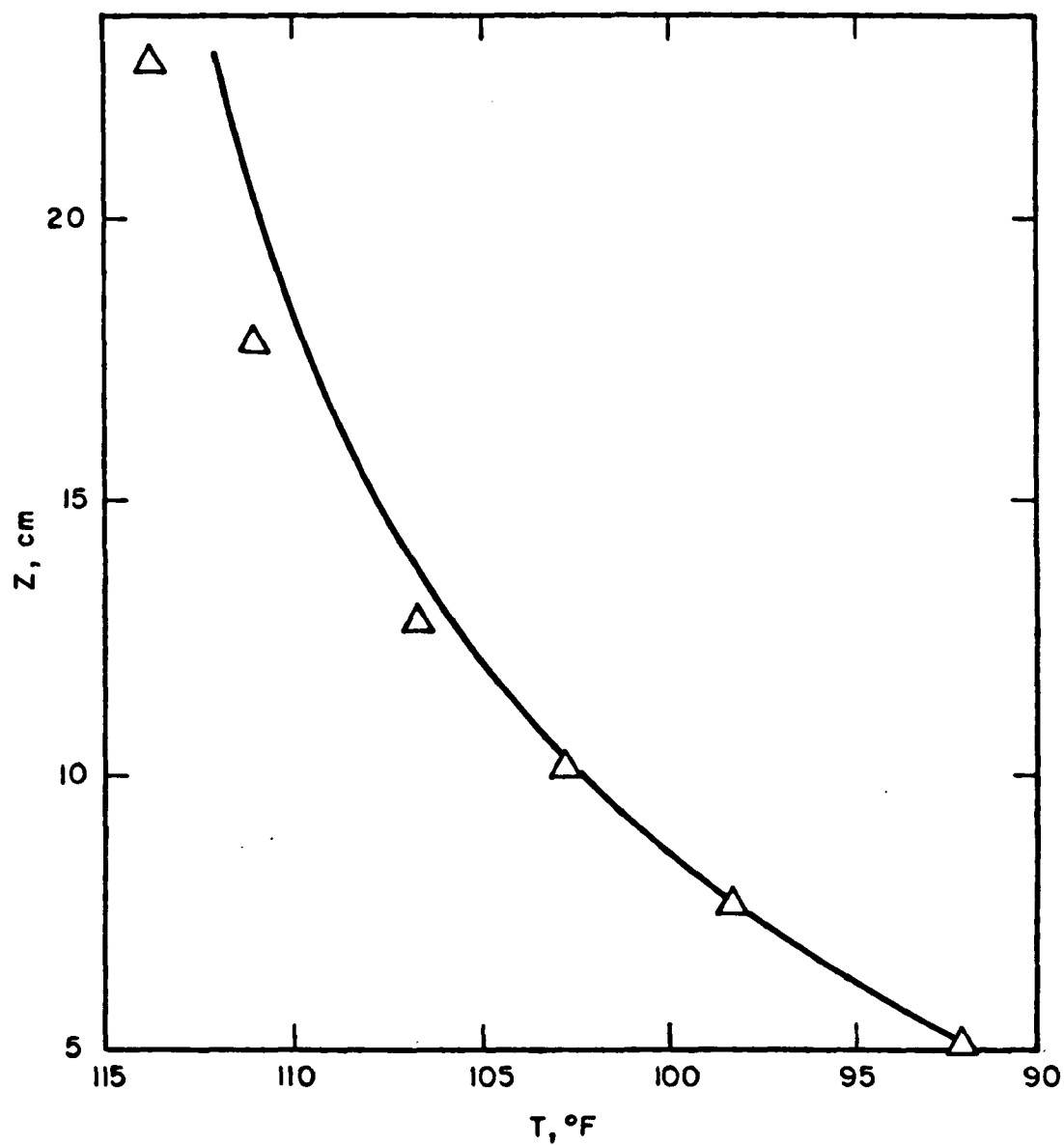


FIGURE 1 COMPARISON OF THE TEMPERATURE PROFILE BETWEEN THE WIND TUNNEL MEASUREMENTS¹⁰ AND THE SABL MODEL CALCULATIONS

Key: — Model calculation; \triangle Arya

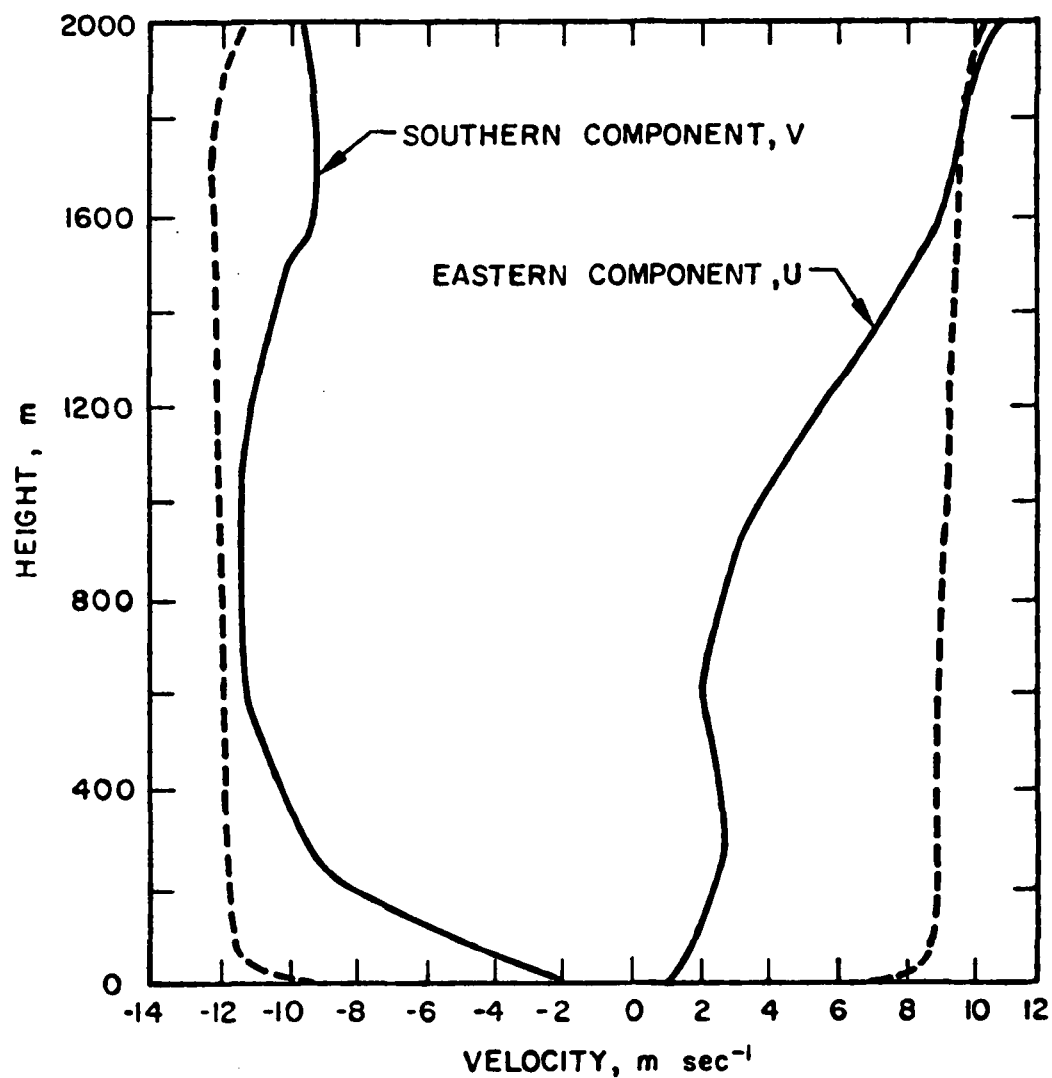
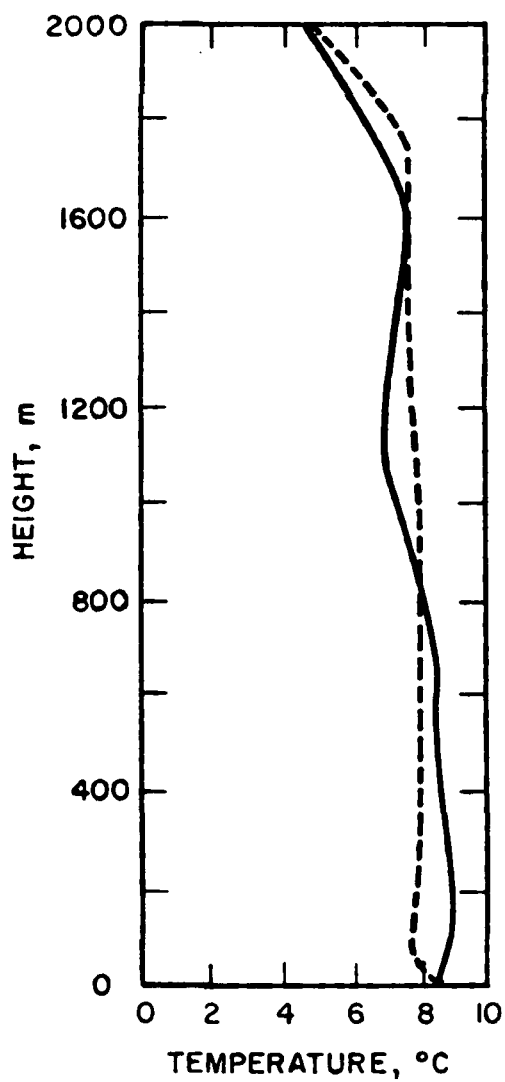


FIGURE 2 COMPARISONS BETWEEN THE PREDICTED WIND VELOCITY AND TEMPERATURE AND THE ACTUAL SOUNDING MEASUREMENTS AT KSC ON 0441 Z, DECEMBER 10, 1974

The sounding measurement on 0211 Z, December 10 is used in the calculation as input.

Key: --- Predicted value; — Actual measurement

IV. DISCUSSION AND CONCLUSIONS

At present, the simulation model which predicts the wind velocity and temperature throughout a horizontal quasi-homogeneous ABL has been developed, coded, and partially evaluated. This model is based on several simplifications, viz., that (1) horizontal advection and horizontal diffusion are not important, (2) the dynamic effects of water (humidity) within the ABL on the buoyant mechanism can be neglected, and (3) radiation and the interactions of large phenomena, e.g., long wave propagations, do not significantly affect the predictions. Although these simplifications are not valid in some meteorological conditions, it is not now clear how much error each simplification can cause, and how important each one is under various meteorological patterns in the KSC area. In other words, appealing to Occam's razor, an extensive verification of the developed model against various meteorological conditions at KSC should be made before attempting to further modify the code to include some of the ignored dynamic features.

As is common in running a theoretical model for realistic problems, some difficulties exist in preparing the input information required to make predictions. In this specific case, problem areas are the geostrophic wind at the surface, the ground temperature (or flux) history over the period covered by the prediction, and the stress near the ground. Although some established theorems to estimate these quantities do exist, these theorems unfortunately require more extensively measured data than are available in most situations. For example, the stress near the ground can be interpolated¹¹ from the local velocity profile near the ground, which is measured from the two tallest towers in the KSC area. Since these two towers are located near the coastline and far from the sounding measurement site, it is doubtful that the stress interpolated from them is the same as that at the sounding measurement site. A higher value for this stress at the towers than at the sounding site can especially be expected in a land/sea breeze condition because such a condition will intensify the turbulence strength and consequently the stress. As in the previous sounding comparisons, the input value of the stress near the ground was that interpolated from the tower measurements at as much as five hours after the time of the start of the calculations. The later (midnight) tower measurements were used because of the lack of tower data at the time desired. Since the land breeze is strongest at midnight, the stress used for the input is certainly higher than it should be; the eastern component of the stress is especially large because the sea is to the east at KSC. Therefore the eastern component of the predicted wind velocity in the comparison shown in Fig. 2 was stronger than the measured values because the higher mandatory input stress enhanced the vertical mixing and smoothed out the velocity differences between the higher and lower levels. Thus it is likely that the predicted value will compare better with the measurement data if more accurate surface stress is used as input.

We had proposed earlier to evaluate the model by comparing it directly with the tower measurements at KSC and the Savannah River plant. Because previous studies⁹ have shown that the Monin-Obukhov theory correlates well with tower data at KSC and the present model provides excellent agreement with the Monin-Obukhov predictions, the comparison between the model results and the KSC tower measurements need not be pursued.

In the present model, the initial value of the turbulent kinetic energy is obtained with the assumption that the total energy production (buoyant and shear production) balances the dissipation. This conflicts with the conclusion drawn from the spectra study of the horizontal turbulence at KSC by Fichtl and McVehil.¹² They have shown that the energy budget indicates a balance of dissipation and shear production only. Buoyant energy production apparently cancels the vertical flux divergence. Some uncertainties remaining in the work of Fichtl and McVehil should be checked before modifying the present model. For instance, the buoyant subrange was not clearly shown in their crude measured spectra.

In conclusion, the present model simulating the ABL at Kennedy Space Center using a simplified second-order closure scheme demonstrates the potential to solve the very complex problem of predicting the behavior of the ABL. The applicability of such an approach should prove quite widespread; further verification and/or refinement of the present model should be encouraged.

The computer code for the simulation model is stored in the computer facility at NASA/Langley.

V. REFERENCES

1. Hwang, B.C., "First Quarterly Technical Letter Progress Report on 'A Simulation Model of the Planetary Boundary Layer at Kennedy Space Center,' Covering the Period 27 June to 30 September 1977," AeroChem TL-870, 11 October 1977.
2. Hwang, B.C., "Second Quarterly Technical Letter Progress Report on 'A Simulation Model of the Planetary Boundary Layer at Kennedy Space Center,' Covering the Period 1 October to 31 December 1977," AeroChem TL-883, 26 December 1977.
3. Rotta, J.C., "Statistische Theorie nichthomogener Turbulenz," Z. Phys. 129, 547 (1951); 131, 51 (1951).
4. Kolmogoroff, A.N., "The Equations of Turbulent Motion in an Incompressible Fluid," Izv. Akad. Nauk SSSR, Ser. Fiz. 6, 56 (1942).
5. Mellor, G.L. and Herring, H.J., "A Survey of Mean Turbulent Field Closure Models," AIAA J. 11, 590 (1973).
6. Mellor, G.L. and Yamada, T., "A Hierarchy of Turbulence Closure Models for Planetary Boundary Layers," J. Atmos. Sci. 31, 1791 (1974).
7. Yamada, T. and Mellor, G., "A Simulation of the Wangara Atmospheric Boundary Layer Data," J. Atmos. Sci. 32, 2309 (1975).
8. Mellor, G. and Yamada, T., "A Turbulence Model Applied to Geophysical Fluid Problems," Princeton University, 1977 (preprint).
9. Blackadar, A.K., "The Vertical Distribution of Wind and Turbulent Exchange in Neutral Atmosphere," J. Geophys. Res. 67, 3095 (1962).
10. Arya, S.P.S., "Structure of a Stably Stratified Boundary Layer," PhD. Thesis, College of Engineering, Colorado State University, Fort Collins, Colorado, 1968.
11. Hwang, B.C., "Rocket Exhaust Ground Cloud/Atmospheric Interactions," Final Report, AeroChem TP-362a, NASA CR-2978, December 1977, Section V.B.
12. Fichtl, G.H. and McVehil, G.E., "Longitudinal and Lateral Spectra of Turbulence in the Atmospheric Boundary Layer at the Kennedy Space Center," J. Appl. Meteor. 9, 51 (1970).